ELECTROMAGNETIC AND MECHANICAL PROPERTIES OF NIOBIUM CAVITIES
FOR A SUPERCONDUCTING ELECTRON LINEAR ACCELERATOR*

W. B. Herrmannsfeldt, R. H. Helm and R. R. Cochran
Stanford Linear Accelerator Center
Stanford University, Stanford, California 94305

ABSTRACT

This paper describes the computer studies of the electromagnetic and mechanical properties of an S-band superconducting accelerator. The structure under discussion is intended for a test accelerator using a 15-cavity niobium traveling-wave resonant-ring structure operating in the $2\pi/3$ mode. Many of the parameters for this short test accelerator, such as the frequency (2856 MHz) and the accelerating field (33 MV/m), are the same as those proposed for the possible conversion of the SLAC two-mile long linear accelerator.

The electromagnetic studies were made to optimize the various structure parameters including the quality factor Q, the shunt impedance r, the ratio r/Q, and the ratios of the peak-to-effective electric and magnetic fields. The resulting structure has a slight bulge at the disk tip and an elliptical cross section at the outer wall. The calculated values for the peak field ratios are $\hat{E}/E_{eff}=1.66$ and $\hat{H}/E_{eff}=31\,G/(MeV/m)$. The paper includes a comparison of these and other parameters for different modes between $\pi/2$ and π.

The mechanical studies were made to determine the frequency shifts due to deflection of the walls by the rf fields. Changes were made to the mechanical design and to the fabrication techniques during the study to minimize these frequency shifts.

Introduction

This paper presents the results of a design study for a superconducting accelerator structure with the goal of providing the optimum cavity shape for a high energy electron accelerator. The parameters were chosen according to the plan described by Loew and Neal[1] to build a prototype of the structure that would be used to convert the SLAC two-mile accelerator to a 100 GeV superconducting accelerator. The choice of frequency, 2856 MHz, is based on a study[2,3] which showed that substantial cost savings would result if the new accelerator operated at the same frequency as the present room temperature structure.

The structure optimization was based on the principle that maximum accelerating field is the most important criterion. Improvements in the cavity quality factor Q, or in shunt impedance r, while desirable, are considered of secondary importance since these parameters relate to refrigeration load and/or duty cycle. A number of factors are involved in optimizing the design. There are the obvious structure parameters; e.g., the mode, beam aperture, and frequency. Fabrication techniques must be considered especially as to the number and type of welds needed. Wall thickness is important because superconducting niobium is a very poor thermal conductor. An increase of temperature of $0.1\,^{O}K$ causes about a factor of 2 loss of Q. Thickness also affects cost and adds to the difficulty of some fabrication techniques. If the wall

---

is too thin it is hard to maintain tolerances during fabrication. In addition the deflection of the walls by the rf fields has been considered in some detail. This is a phenomenon which has not been significant before the advent of these high-field, high-Q cavities.

General Considerations of High Field Intensity

The limitations on the accelerating field in a superconducting accelerator structure are quite different from the limitations encountered when considering a room temperature structure. In fact, in a normal or room temperature structure, it is usually the available rf power which limits the accelerating field rather than the design of the structure itself. However, since the basic idea of a superconducting accelerator is that nearly all the rf power is available to accelerate the beam, it is almost inevitable that the power is sufficient to excite fields to the limits imposed by the structure itself. In the case of a normal structure, one generally is only concerned with the maximum electric field. When field emission occurs in the normal structure, the usual result is the emission of some radiation and, in a severe case, an increase in the pressure. But for a superconducting accelerator structure, either the electric field or the magnetic field may limit the accelerating structure. The magnetic field is limited by the magnetic breakdown field of a superconductor. This is the rf field which if applied at the surface of a superconductor produces a critical power dissipation that forces some local area to become normal. This magnetic breakdown field is less than H_c, the critical field at which flux starts to penetrate the superconductor. When the magnetic breakdown field is locally exceeded, the rf losses rise drastically preventing further cavity excitation. For niobium cavities the highest rf magnetic fields achieved to date are about 1000 gauss by Turneaure and Viet.[4] Since this paper is primarily concerned with the application of the empirical results, the reader who is interested in the experimental background and a possible interpretation is referred to the paper by Rabinowitz[5,6] and the references cited there. For the purposes of this study, it has been assumed that the goal of 1000 gauss will be achievable in production when enough has been learned about processing techniques.

The situation regarding maximum electric field is even less clear cut. The superconducting structure will emit radiation just as described above for a normal cavity. However, most of the energy which is coupled to field emission electrons will end up as heat in the cavity walls. In mild cases, this heat adds to the load on the refrigeration system. It thus represents a reduction in Q. In severe cases, field emission could also damage the surface, possibly leading to the growth of "whiskers" which further cause more field emission.

It has been assumed that macroscopic as well as microscopic surface conditions affect the electric and magnetic field limits. Thus, for example, high quality machining followed by at least one chemical etching and at least one high-temperature high-vacuum firing has been considered the minimum conditions for success. Joints, where necessary, have been made by electron-beam welding in the most successful cavities.[4,7] These welds have been made from the outside wall with particular attention to avoiding regions of high electric or magnetic field. However, repeated tests of the welding process have shown the following:

1. If the welding power is insufficient, the weld does not penetrate and a small crack will remain on the inner wall.

2. If the beam power is increased there is danger of spiking through and sputtering some material around on the inside of the cavity.

On the other hand, if the weld can be made from the inside, much less power is required and very smooth welds are possible. Figure 1 shows an example of an inside weld and Fig. 2 shows an outside weld, both viewed from the inside. Structurally, the best combination appears to be to weld both the inner and outer surfaces with relatively low power. This approach has an added benefit that it holds dimensional tolerances better than a single high power weld. Welding the inside surface is possible if the sequence of assembly operations is correctly planned. Although inside welds have yet to be tried in test cavities, there is every hope that they will have good rf properties. This is especially important since the trick of avoiding welds in regions of high field appears to be difficult in real accelerator cavities.

The choice of fabrication technique is between machining from solid material and some method of forming from sheet material. For the fairly small cavities required at 2856 MHz, it appears that coining is the best method of fabrication. The coining technique uses a closed die so that the edges are completely formed at the same time as the cavity is shaped. The surface finish that results is as good as the finish on the die. Although there is an initial investment in the set of dies, it is estimated that the total cost will be less than for other forming methods even for a short prototype accelerator consisting of as few as 30 half-cavity shells. This is because of the extra machining required on each piece in any competing scheme.

The major difficulty with any thin-walled structure is maintaining tolerances both during assembly and in operation. A cavity machined from solid niobium would be much more stable but it would be necessary to machine some sort of "honeycomb" of passages to permit adequate cooling.

With the use of a thin wall structure it becomes necessary to consider wall deformations due to the rf fields. The wall deformations that are expected at high fields are sufficient to detune these high-Q structures. The tuning system, which must correct for this shift, has a fairly narrow range and thus restricts the amount of detuning permitted. The calculations of wall deformations and the detuning which results is described later in this paper. The design of the cavity, and even the choice of fabrication technique, was affected by the results of those calculations. Generally, it was found that the frequency was especially sensitive to deflections at the tip of the disk. Since the magnetic fields are lowest at the disk tip (the deflection at this point is due to the electric field) the rf losses are also low so that it is possible to make the disk thicker at the tip. In fact, it was found that a solid disk tip is required. This determination led to the decision, described earlier, to coin the cavity parts since the solid tip would have to be coined anyway or machined separately if the rest of the cavity were to be formed in some other way.

Structure Optimization Studies

General Considerations

As has been stated previously, the primary objective in optimizing the superconducting structure is to minimize the ratios $\hat{E}/E_{eff}$ and $\hat{H}/E_{eff}$ where $\hat{E}$ and $\hat{H}$ are the peak electric and magnetic fields on the conducting surfaces. E_{eff} is the effective acceleration field. Shunt impedance and Q are less important because the rf power requirement is dominated by beam loading, not wall losses.

The peak electric field ($\widehat{E}$) always occurs near the disk aperture. When the disk edge has circular rounding as in the existing SLAC structure, this peak usually occurs well out on the round edge, perhaps 70° to 80° from the inner tip, while the electric field at the tip may be 40% or 50% lower than $\widehat{E}$. This suggests that the rounding of the disk edge should increase in radius of curvature as one goes outward from the tip. Thus the profile of the disk edge should resemble a convex ellipse with the long axis in the radial direction. It would also be desirable to increase the thickness of the disk at least near the tip, so that the radius of curvature could be even greater.

The peak magnetic field ($\widehat{H}$), usually occurs on the disk somewhat inside the outer wall radius. The magnetic field along the outer wall may be on the order of 20% lower than the peak. By using a suitably rounded, rather than right-angled, outer cavity profile, the peak is spread out somewhat and also the volume-to-surface ratio may be improved; these effects can decrease the peak magnetic field (and incidentally improve the r_0 and Q). Going to thinner disks also tends to decrease the magnetic field by increasing the volume available for stored magnetic energy.

Decreasing the disk aperture tends to improve both $\widehat{E}/E_{eff}$ and $\widehat{H}/E_{eff}$ by improving the transit-angle factor. Note, however, that "nose cones" of the Los Alamos type,[8] which also improve the transit angle factor, have the effect of increasing $\widehat{E}$ because the electric field lines become concentrated on the tip of the nose.

It will be seen that requirements for minimizing $\widehat{E}/E_{eff}$ and $\widehat{H}/E_{eff}$ are to some extent conflicting. If one tries to reduce $\widehat{E}/E_{eff}$ by making a pronounced bulge on the disk tip, then $\widehat{H}/E_{eff}$ increases because the volume available for stored magnetic energy is reduced. On the other hand, if the wall profile is optimized with respect to $\widehat{H}/E_{eff}$, the disk tip becomes quite thin, resulting in high $\widehat{E}/E_{eff}$. A reasonable compromise seems to be to try to reduce the electric field as much as possible without increasing magnetic field significantly from the best attainable value.

Several arbitrary restraints have been placed on the SLAC design study. First, it is assumed that the frequency will be 2856 MHz. Second, the disk aperture is to be at least 1.0 cm radius because of beam transport consideration. Third, the minimum disk thickness should be about 0.6 cm to permit adequate wall thickness while still allowing space for refrigerant slots.

Computer Programs

The design study has been aided by two programs: the Los Alamos program LALA[8,9] which has been adapted to run on the IBM 360/91 at SLAC; and a traveling wave program (TWAP) developed at SLAC.[10] LALA, which does a standing wave computation, does not yield directly the traveling wave values of peak fields and shunt impedance, does not give group velocity, and is restricted to a few values of phase shift per cell such as $\pi/2$, $2\pi/3$ and π. The calculation of traveling wave peak fields and shunt impedance from the standing wave values is described elsewhere.[11] TWAP has the advantages of computing the traveling wave values, including group velocity, for arbitrary phase shift. The two programs agree fairly well in cases where comparison is possible.

Leapfrog Design

The design of the fifteen cell test accelerator, "Project Leapfrog",[1] was based on a simple model in which the cell profile consists of two tangent ellipses. Figure 3 shows the geometry and nomenclature. Preliminary computer runs showed that $\widehat{E}/E_{eff}$ is minimized when b_1/a_1 (elongation of disk tip profile) is approximately 2:1. For a few different values of the tip thickness a_1, the angle α (slope at the tangent point) was varied, with appropriate adjustment of a_2 and b_2 to correct the frequency. The mode was kept fixed at $2\pi/3$. It was found that the following set of parameters gave quite good results:

$$\ell = 3.5000 \text{ cm} \qquad b = 4.4000 \text{ cm}$$
$$a = 1.0000 \text{ cm} \qquad t = 0.2857 \text{ cm}$$
$$a_1 = 0.4000 \text{ cm} \qquad a_2 = 1.4643 \text{ cm}$$
$$b_1 = 0.8000 \text{ cm} \qquad b_2 = 1.7109 \text{ cm}$$
$$\alpha = 75^{\circ}$$

Figure 4 shows one and one-half cells of this structure drawn to scale.

Table I shows the rf properties of this structure as computed by LALA and TWAP. The "tapered disk" structure shown for comparison is another example of the two-ellipse model but

TABLE I

Computer Results for $2\pi/3$ Copper Structures

	Leapfrog		Tapered Disk	
	LALA	TWAP	LALA	TWAP
f(MHz)	2856.6	2858.1	2856.2	2856.0
Q	15,149	15,040	14,493	14,460
r (MΩ/m)	65.9	65.4	60.8	59.7
$\widehat{E}/E_{eff}$	1.65	1.61	1.75	1.66
$\widehat{H}/E_{eff}$ [G/(MeV/m)]	30.5	30.2	30.9	31.1
r/Q (Ω/cm)	43.4	43.5	42	41.3
v_g/c		0.0071		0.0078

with $a_1 = 0.3$ cm, $b_1 = 0.6$ cm, and $\alpha = 90^{\circ}$. This structure is illustrated in Fig. 5.

A test stack consisting of six machined brass cells was built according to the Leapfrog dimensions. Table II compares the experimental[12] and computed frequencies and group

TABLE II

Experimental and Computed Frequencies and Group Velocities in Leapfrog Test Stack

	Frequency, MHz			v_g/c	
Mode	Experiment	LALA	TWAP	Experiment	TWAP
0	2843.969	2841.08	2841.29	0	0
$\pi/6$	2845.092	–	2842.80	.00398	.00412
$\pi/3$	2849.398	2848.13	2846.91	.00715	.00713
$\pi/2$	2854.946	2851.38	2852.51	.00818	.00820
$2\pi/3$	2860.542	2856.56	2858.10	.00692	.00709
$5\pi/6$	2864.377	–	2862.17	.00405	.00408
π	2866.077	2862.09	2863.66	0	0

velocities for several modes in this test stack. The systematic discrepancy in frequency is not understood but may indicate an error in the specifications for the mechanical fabrication. The random part of the differences results at least in part from machining errors; the 6 individual cells were found to differ one from another by over 1 MHz in frequency.

The values of r_{tot}/Q for the $2\pi/3$ mode are:

Experiment: 53.49 Ω/cm   TWAP: 53.33 Ω/cm   LALA: 53.66 Ω/cm

Here r_{tot} is the shunt impedance found experimentally by perturbing the cavity with a long dielectric rod. The experimental value of r_0/Q (where r_0 is the synchronous shunt impedance) was not determined; see Table I for computed values.

Effect of Phase Shift

The results of a preliminary survey of properties vs phase shift per cell is shown in Table III. These calculations were all based on the "tapered disk" design, that is, the two ellipse

TABLE III

TWAP Results vs Phase Shift per Cell for Copper Structures

kℓ	$\pi/2$	$2\pi/3$	$3\pi/4$	$5\pi/6$	π
$\ell/2$ (cm)	1.3125	1.7500	1.9687	2.1875	2.6250
b (cm)	4.7213	4.6851	4.6696	4.6549	4.6259
r/Q (Ω/cm)	44.2	41.3	38.6	35.5	28.6
Q	10,770	14,460	16,090	17,590	20,250
r (MΩ/m)	47.6	59.7	62.2	62.5	57.9
v_g/c	.00925	.00784	.00630	.00437	0
$\hat{E}/E_{eff}$	1.561	1.661	1.768	1.884	2.096
$\hat{H}/E_{eff}$ [G/(MeV/m)]	31.5	31.1	31.5	32.3	35.2

model of Fig. 5 with $\alpha = 90°$. The parameters were a = 1 cm, $a_1 = 0.3$ cm, $b_1 = 0.6$ cm; ℓ and b were chosen to give phase velocity v_p = c at 2856 MHz. The best case seems to be somewhere between $\pi/2$ and $3\pi/4$, depending on whether $\hat{E}$, $\hat{H}$ or r_0 is the most critical parameter.

Further Optimization

Further studies are proceeding with the aid of slightly more complicated models which permit more independent minimizing of $\hat{E}$ and $\hat{H}$. Preliminary indications are that structures at least as good in $\hat{H}$ and appreciably better in $\hat{E}$ are possible in both the $2\pi/3$ and $3\pi/4$ modes. The latter case could prove quite attractive since fewer welds and less material would be required.

Deformation Due to Rf Fields

With the interest in high-field, high-Q structures, particularly with thin walls, it becomes important to consider the frequency shift due to wall deformations caused by the rf fields themselves. Such frequency shifts will produce small changes in the phase shift per cavity and cause the ring to drop slightly out of resonance. The tuning system, which must correct for this shift, has a narrow range and thus restricts the amount of detuning permitted. The pressures on the

walls are found from the fields calculated by LALA. The RMS pressure is,

$$P_{RMS} = 1/4 \left(\mu_0 H^2 - \epsilon_0 E^2 \right)$$

where H and E are the peak fields in the traveling wave mode. The work done, δW, is found by integrating the pressure over the small volume of distortion, τ,

$$\delta W = 1/4 \int_\tau \left(\mu_0 H^2 - \epsilon_0 E^2 \right) d\tau$$

The frequency shift is related to this quantity δW by the Slater perturbation formula[13]:

$$\delta\omega/\omega = - \delta W/U$$

where U is the total stored energy in the cavity in the traveling wave mode given by

$$U = 1/4 \int_V \left(\mu_0 H^2 + \epsilon_0 E^2 \right) dV \ .$$

The work, δW, was found by a numerical integration over the surface

$$\delta W = \sum_S (P_i A_i) \ \delta x_i$$

where P_i equals average pressure over the element of area A_i and δx_i equals the calculated deformations in the direction of the applied pressure.

The deformations were calculated by NONLIN,[14] a program developed by Battelle Memorial Institute, to investigate stresses and deformations in bellows. NONLIN solves the differential equations describing the behavior of thin walled shells by direct segmental numerical integration. It accepts both variable loading and variable wall thicknesses as well as several different shell shapes. Since, compared to most bellows, accelerator cavities are thick walled shapes, there was some fear that NONLIN would not give accurate results. Wall deflections of "standard" shapes with several different wall thicknesses were calculated using NONLIN. The results for these simple shapes agreed with handbook formula results even for fairly thick walls giving confidence in the validity of the cavity calculations.

The first cavities analyzed had walls about .050" thick. The calculated detuning was unacceptably large and the wall thickness was increased to 0.100". This design has a predicted frequency shift of 234 Hz. Since large deflections occurred near the maximum radius of curvature — where two adjacent cavities are closest to each other — a stiffener ring was added between adjacent cavities. Surprisingly, this did not result in a significant reduction of the frequency shift.

A closer look revealed that this area of large deflection coincided with a low field region and thus had nowhere near the effect that the higher electrical fields had in conjunction with the relatively small deflection of the disk tip. Up until this time the most likely method of fabrication of a small test accelerator involved a process for forming a shape with uniform wall thickness. The calculations suggested a look at stiffening the disk tip, so three types of solid tips were analyzed. The first, solid to the point of closest proximity of the two cavities, has a calculated frequency shift of 125 Hz. The second, solid to the inflection point between the large ellipse and the tip ellipse has a frequency shift of 145 Hz. The third, solid to the center of the tip ellipse, has a frequency shift of 147 Hz. The latter design was selected since the added

fabrication complications posed by the other designs were not justified by the small improvement in stability.

At this time the design consisted of a formed uniform wall shell attached to a solid, machined disk tip. Several niobium test cavities were fabricated in this manner. However, it was becoming more apparent that the only economical way to make these parts in quantity, to the required accuracy, would be by coining. An investigation of relative costs showed that coining was reasonable even for the small test accelerator. Since considerable freedom in configuration is allowed by the coining process, the design was modified to that shown in Fig. 6. The frequency shift predicted for this latest shape is 107 Hz. The wall deflections calculated for the uniform .100" thick wall design and the latest configuration are shown in Fig. 7. By comparison, the calculated frequency shift due to a change in external pressure by 1 Torr is 13 Hz.

Acknowledgements

The authors wish to acknowledge the contributions to this study made by other members of the group working on the Leapfrog project; notably R. H. Miller, P. B. Wilson, H. Hogg, G. A. Loew and A. V. Lisin. G. Fritzke made the photographs of the electron-beam welds.

References

1. G. A. Loew and R. B. Neal, "Recent and planned improvements of conventional electron linacs," Invited paper presented to the 1970 Proton Linear Accelerator Conference, NAL, Batavia, Illinois.

2. Feasibility Study for a Two-Mile Superconducting Accelerator, Stanford Linear Accelerator Center (December 1969) limited distribution. A review of this study appears in Ref. 3.

3. W. B. Herrmannsfeldt, G. A. Loew and R. B. Neal, "Two-mile superconducting accelerator study," presented at the 7th International Conference on High Energy Accelerators, Yerevan, Armenia, USSR, August 27 to September 2, 1969; available as Report No. SLAC-PUB-626, Stanford Linear Accelerator Center (July 1969).

4. J. P. Turneaure and N. T. Viet, Report No. HEPL-612, High Energy Physics Laboratory, Stanford University (October 1969).

5. M. Rabinowitz, "Critical power dissipation in a superconductor," Appl. Phys. Letters 16, 419 (1970).

6. M. Rabinowitz, "Analysis of critical power loss in a superconductor," Paper presented at the Fourth Applied Superconductivity Conference, Boulder, Colorado, June 1970. Available as Report No. SLAC-PUB-714, Stanford Linear Accelerator Center. To be published in J. Appl. Phys. January 1971.

7. P. B. Wilson and M. Allen, Stanford Linear Accelerator Center, private communication.

8. H. C. Hoyt, D. D. Simmons and W. F. Rich, "Computer designed 805 MHz proton linac cavities," Rev. Sci. Instr. 37, 755 (1966).

9. W. F. Rich and M.D.J. MacRoberts, "Numeric solution of the fundamental mode of cylindrically symmetric resonant cavities," Report No. LA-4219, Los Alamos Scientific Laboratory, Los Alamos, New Mexico (September 1969).

10. R. H. Helm, "Computation of the properties of traveling wave linac structures," Proceedings of the 1970 Proton Linear Accelerator Conference, NAL, Batavia, Illinois.

11. P. B. Wilson et al. "Superconducting accelerator research and development at SLAC," Particle Accelerators, to be published.

12. H. Hogg and T. C. McKinney, private communication.

13. J. C. Slater, Microwave Electronics (D. Van Nostrand Inc., New York, 1950).

14. T. M. Trainer et al., Final Report on the Development of Analytical Techniques for Bellows and Diaphram Design, Battelle Memorial Institute, Columbus Laboratories, Report No. AFRPL-TR-68-22, Air Force Rocket Propulsion Laboratory, Research and Technology Division, Air Force Systems Command, Edwards Air Force Base, California.
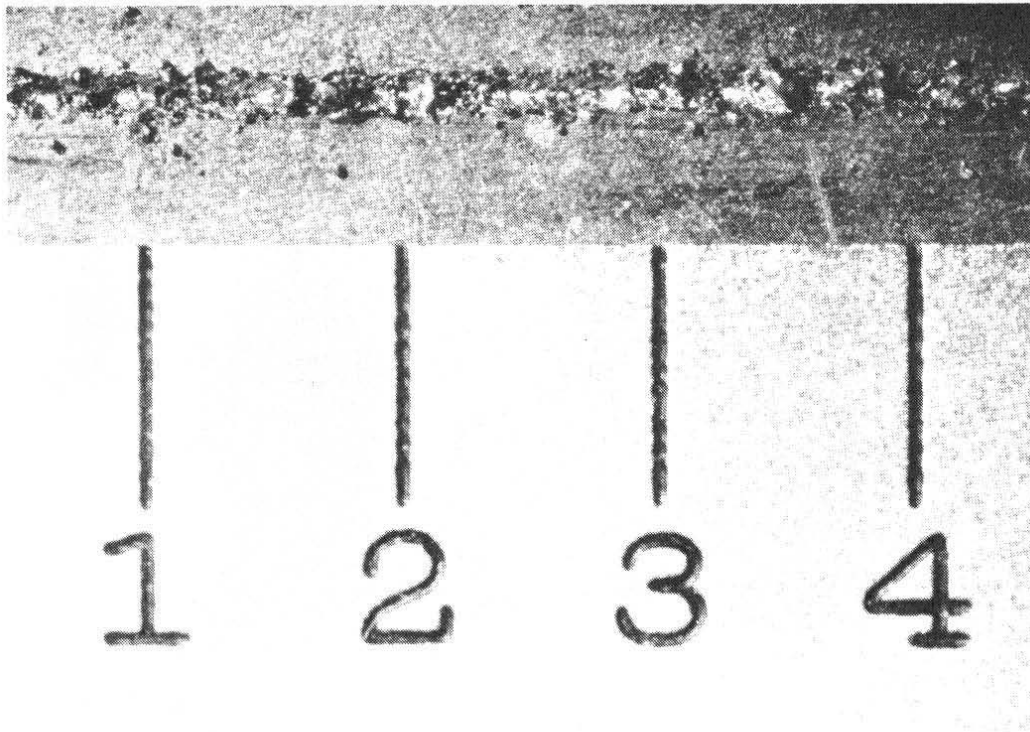
FIG. 1--Photograph of a full-penetration weld from the back side.
This would be the way a typical cavity would look on the
inside after welding from the outside.
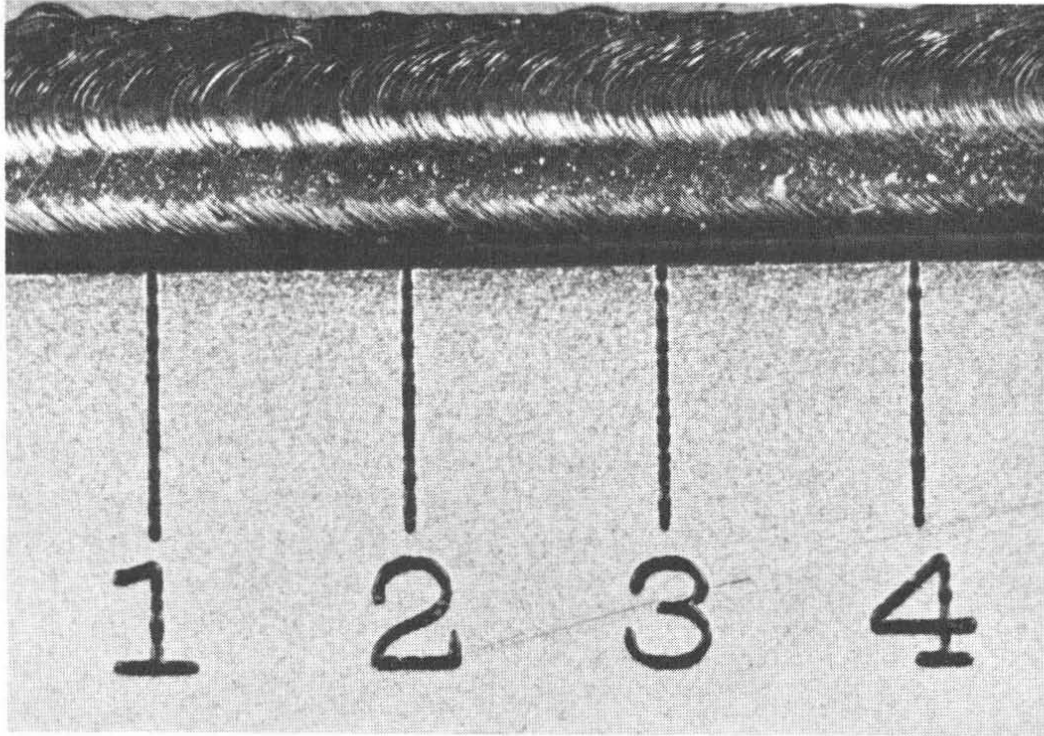
FIG. 2--Photograph of a low-power "cosmetic" weld from the front surface.
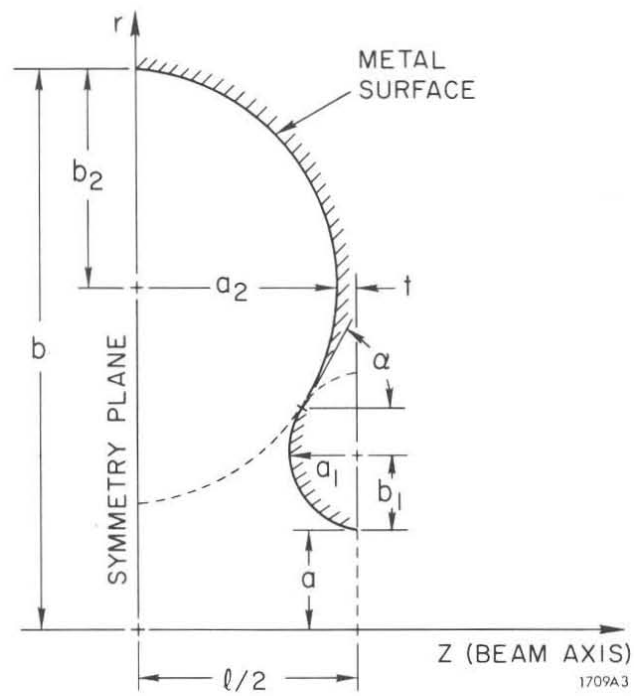
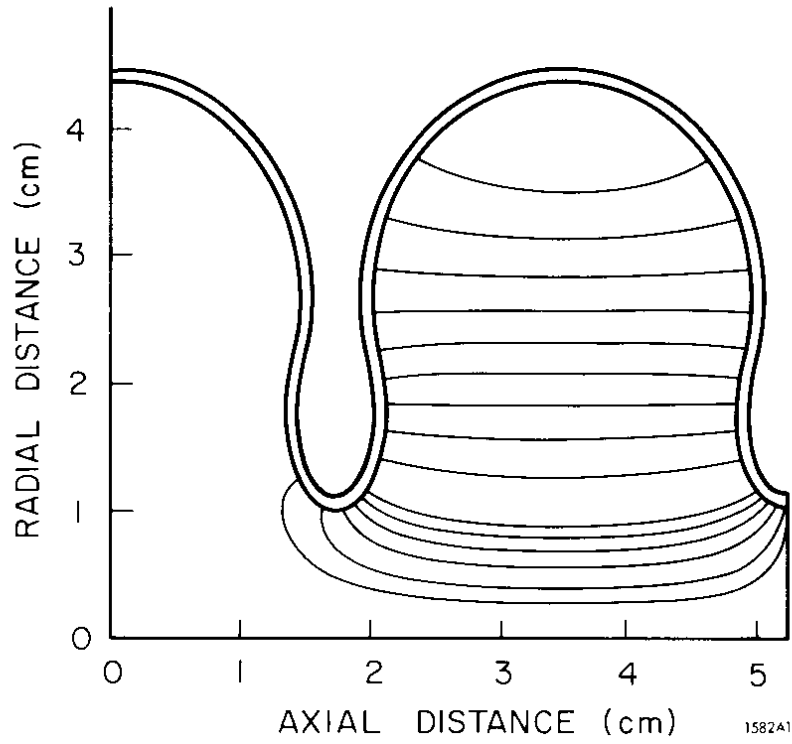

FIG. 3--Geometry of the two-ellipse cell model.

FIG. 4--Cavity planned for the Leapfrog test accelerator.
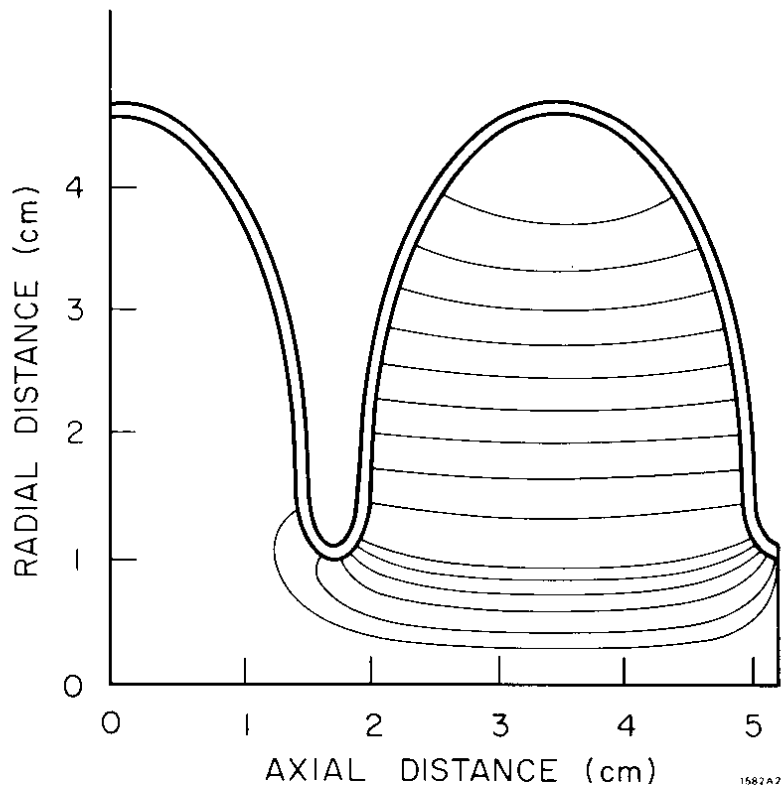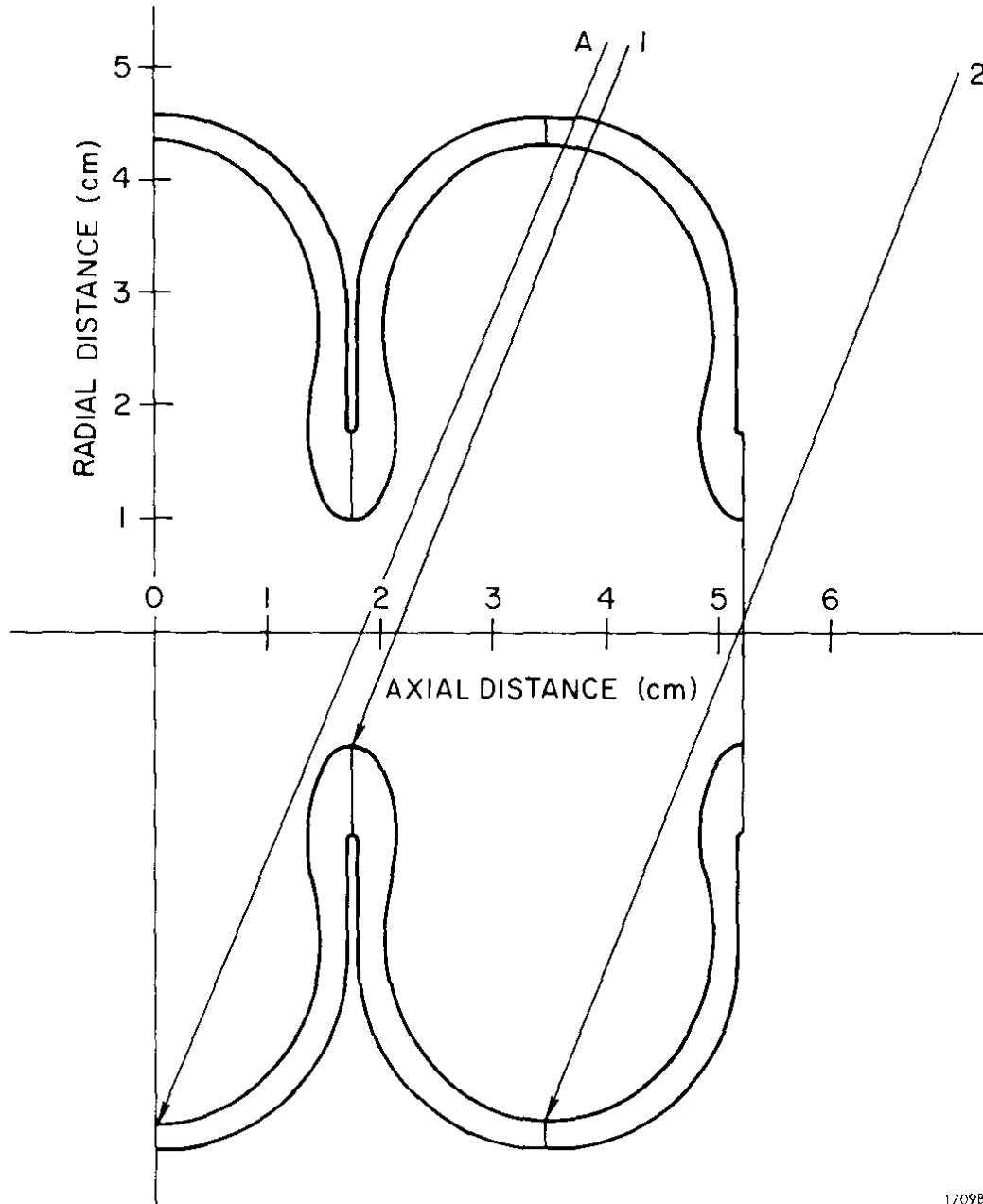Field lines shown are calculated by LALA.

FIG. 5--Tapered disk structure with field lines as
calculated by LALA.

FIG. 6--Section of assembled structure. Lines 1 and 2 are successive beam
paths to weld the structure from half-cavity shells. Line A is the
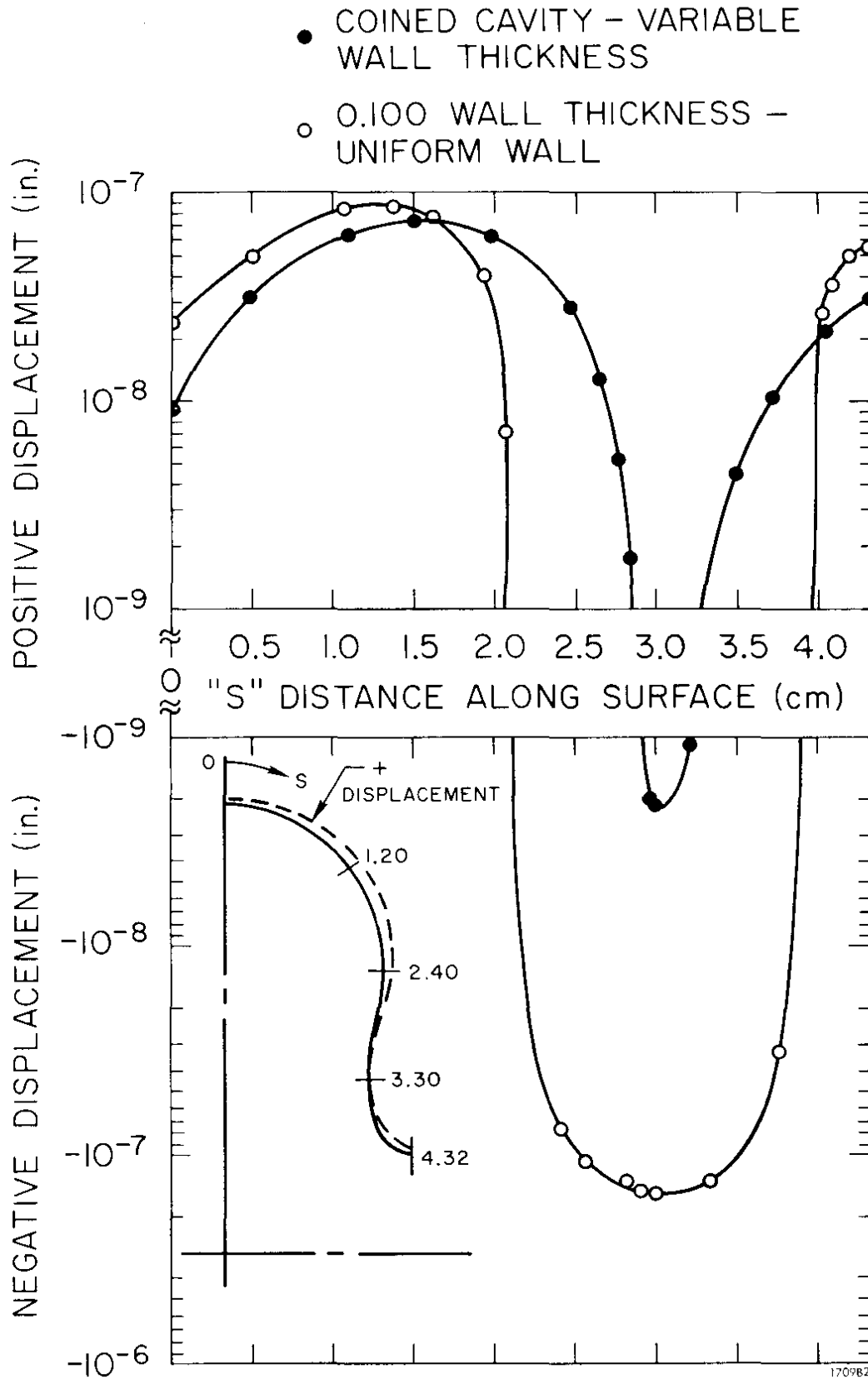path required if the structure is to be assembled from full-cavity
sections.

FIG. 7--Wall deflections of the Leapfrog structure with a wall thickness of 0.075 in. and a guard tube of 0.050 in. thick niobium.